18PB-019

Development of Long Pulse Beam Acceleration for ITER Negative Ion Beam
ITER 級負イオンビームの長パルス加速開発

Naotaka Umeda, Atsushi Kojima, Junichi Hiratuka, Mieko Kashiwagi, Hiroyuki Tobari, Kazuhiro Watanabe and Masaya Hanada
梅田尚孝、小島有志、平塚淳一、柏木美恵子、戸張博之、渡邊和弘、花田摩砂也

Japan Atomic Energy Agency
801-1,Mukouyama, Naka-shi, Ibaraki-ken 311-193, Japan
日本原子力研究開発機構　〒311-0193　茨城県那珂市向山801-1

To realize high power and long pulse negative ion beam required in ITER, a Multi-Aperture and Multi-Grid (MAMuG) accelerator has been developed in JAEA. A new ion extractor which has reinforced cooling capability and improved beam transparency has been developed in five stage accelerator to extend pulse duration time at a high power density beam. The beam current increased 10 % and total acceleration grid heat load reduced to 1/10 of input electric power. As the results, a long pulse beam acceleration up to 60 s which is the power supply limit, has been achieved at 683 keV, 100 A/m^2 of negative ion beam.

1. Introduction

To realize ITER neutral beam injector (NBI), development of a high power density negative ion accelerator is a key issue. Acceleration of 40 A (200 A/m^2) D$^-$ ions at the energy of 1 MeV for 3,600 s is required for the ITER accelerator. [1] Japan Atomic Energy Agency (JAEA) has developed a Multi-Aperture and Multi-Grid (MAMuG) accelerator called as MeV accelerator for ITER NBI.[2] A target of the MeV accelerator is to accelerate the H$^-$ ion beam of 200 A/m^2 up to 1 MeV for 60 s.[3] The performance of the accelerator has been progressed and the negative ion beam acceleration of 980 keV, 185 A/m^2 for 0.4s was achieved in 2011.[4]

After the high power beam acceleration, R&D for long pulse beam acceleration has started. The main issue for long pulse acceleration is to reduce heat loads on the acceleration grids. It was found that the main part of the grid heat load was due to direct interception of the negative ions onto the acceleration grids. To reduce the heat loads, beam deflection by the residual magnetic field was compensated with aperture offset of an electron suppression grid (ESG). By the correction, long pulse acceleration up to 9 s had achieved at 881 keV, 130 A/m^2.[5] To extend pulse duration time furthermore, modifications of extractor have carried out.

2. MeV accelerator

Figure 1 shows a cross sectional view of the MeV accelerator. The MeV accelerator is composed of a source chamber, an extractor and an accelerator. The source chamber is cesium seeded arc driven kamaboko source whose radius is 170 mm and length is 340 mm. Extractor is composed of three grids such as a plasma grid (PG), an extraction grid (EXG) and ESG. In the PG, 3 x 5 apertures whose diameter is 14 mm are opened to extract negative ions. In the EXG, permanent magnets are embedded to remove co-extracted electrons from the negative ion beam. Several kilovolts of DC voltage is applied between the PG and the EXG to extract negative ions. ESG aperture is off–axis against the EXG to compensate beam deflection by magnetic field. The accelerator is electro-static five stage accelerator. The same acceleration voltage up to 200 kV is applied to each acceleration stage. The EXG and all acceleration grids are cooled by water and heat load of each grid was measured from water temperature rise. Accelerated negative ion beam is dumped on a water cooled copper plate and the beam current is measured from the water temperature rise.

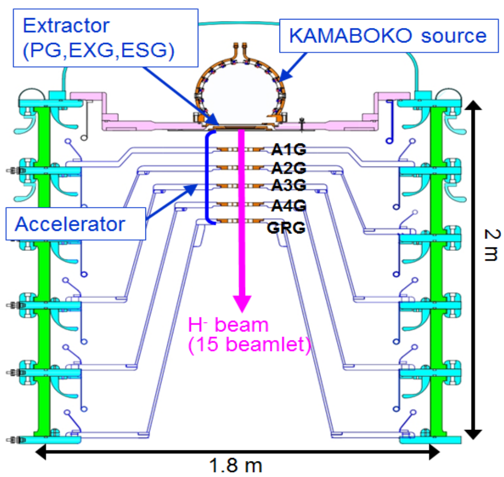

Fig 1 Cross sectional view of the MeV accelerator

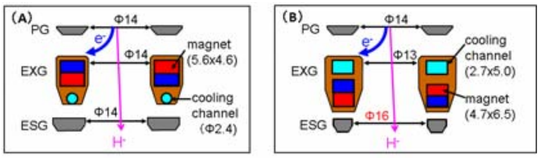

Fig. 2 Cross section of the original extractor (A) and the new extractor (B)

3. Modification of the extractor

The extractor has been modified as shown in fig.2 to extend pulse duration and to increase beam efficiency. One modification is to reinforce cooling capability of EXG to keep magnet temperature lower than 200 degree to prevent magnetic field weakening. The larger cooling channel was set at upper stream of the magnet. Other modification is enlarging the ESG aperture from 14 mm to 16 mm, since a part of negative ion of high current beam intercepted on ESG and many secondary electrons which increases heat loads in the accelerator were emitted.

Figure 3 shows accelerated negative ion current for the new and the original extractors as a function of arc power at constant acceleration and extraction voltage. For the original extractor, the negative ion current increased and saturated around 260 mA at the arc power of 18 kW. For the new extractor,

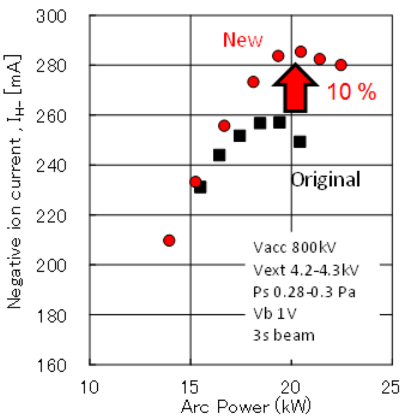

Fig. 3 Comparison of accelerated negative ion current for the original and the new extractor.

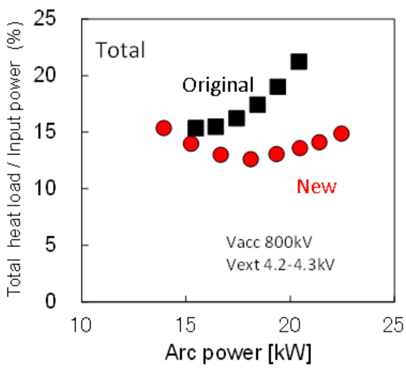

Fig. 4 Comparison of acceleration grid heat load for the original and the new extractor

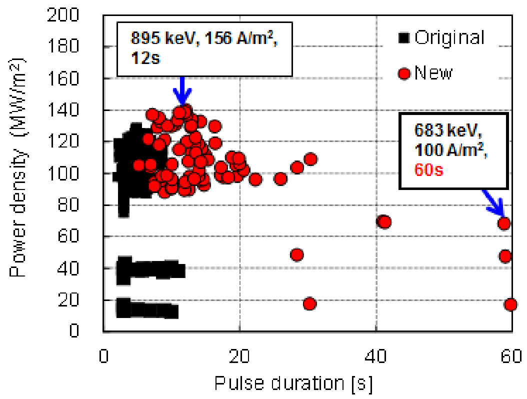

Fig. 5 Long pulse beam acceleration at high power density beam.

the negative ion current increased up to 285 mA at 20 kW and increased by 10 % compared to the current from the original extractor. Figure 4 shows the total acceleration grid heat load divided by electric input power at the same operation condition shown in fig.3. For original extractor, the grid heat load increased from 15 % with increasing arc power. For the new extractor, the grid heat load decreases to 13 % up to 18 kW arc power and increase at higher arc power. These data show the reduction of negative ion interception on ESG and the secondary electron emission, which leads to high acceleration grid heat load.

4. Long pulse beam acceleration

With the new extractor, a high power and a long pulse beam acceleration has been carried out. Figure 5 shows the result. For original extractor, pulse duration time was limited around 10 s. With the modified extractor, the pulse length was extended to the facility limit of 60 s at 683 keV, 100 A/m^2. Beam current and acceleration voltage were very stable during the beam acceleration and water temperature of the acceleration grids reached to steady state. No degradation of beam current and voltage was observed during/after the long pulse beam, and hence the beam energy and pulse duration time is extended with further conditioning toward 1 MeV, 200 A/m^2 for 60 s.

References

[1] ITER EDA Final Design Report, ITER technical basis, Plant Description Document, G A0 FDR 1 01-07-13 R1.0, IAEA EDA documentation No. 24, 2002.

[2] Hemsworth, et. al., Nucl. Fusion **49** (2009) 045006.

[3] T.Inoue, et al., Nucl. Fusion **46** (6), S379-385 (2006).

[4] M.Kashiwagi, et. al., Rev. Sci. Instrum. **83** (2), 02B119 (2012).

[5] N.Umeda, et. al., Rev. Sci. Instrum. **85**, 02B304 (2014)